ELSEVIER

Journal of Molecular Structure (Theochem) 634 (2003) 23–30

THEO CHEM

www.elsevier.com/locate/theochem

# Investigation of the kinetic properties for the forward and reverse WGS reaction by energetic analysis

Guichang Wang[a,*], Ling Jiang[a], Yuhua Zhou[a], Zunsheng Cai[a], Yinming Pan[a], Xuezhuang Zhao[a], Yongwang Li[b], Yuhan Sun[b], Bing Zhong[b], Xianyong Pang[c], Wei Huang[c], Kechang Xie[c]

[a]*Department of Chemistry, Nankai University, Tianjin 300071, People's Republic of China*
[b]*Institute of Coal Chemistry, Chinese Academy of Science, Taiyuan 030001, People's Republic of China*
[c]*Taiyuan University of Technology, Taiyuan 030001, People's Republic of China*

Received 3 January 2003; accepted 27 February 2003

**Abstract**

The kinetic properties of forward water gas shift reaction ($CO + H_2O \rightarrow CO_2 + H_2$) and reverse water gas shift reaction ($CO_2 + H_2 \rightarrow CO + H_2O$) over the copper surface have been analyzed by UBI-QEP approach. For the 'surface redox' mechanism, the energies analysis results show that the rate controlling step in FWGS is the dissociation of adsorbed $H_2O$, and the dissociation of adsorbed $CO_2$ is the rate controlling step of the RWGS reaction. The RWGS reaction is more structure sensitivity than that of FWGS reaction over the Cu single crystal surfaces. Both the activity of FWGS reaction and RWGS reaction over the Cu (111) surface are higher than that of in Au (111) surface. In the meantime, the reason why the FWGS reaction and RWGS reaction is easily poisoned by sulphur has been explained, namely, the activation barrier of rate controlling step increases with the increasing of the coverage of sulphur.


*Keywords:* Models of surface kinetics; Surface energy; Catalysis; Copper; Carbon dioxide; Carbon monoxide; Hydrogen molecule

## 1. Introduction

The high efficiency of the water gas shift (WGS) reaction ($CO + H_2 \rightarrow CO_2 + H_2$) in the production of hydrogen, it has been widely used in the industry [1]. Copper/zinc oxide is frequently used to catalyze this reaction, since this catalyst can be operated at relatively low temperature (473–523 K) [2,3]. Interestingly, this catalyst is also used for methanol synthesis, where the water gas shift reaction is thought to play an important role in the mechanism [2,3]. Although numerous studies of the froward water gas shift reaction (named as FWGS) and the reverse water gas shift reaction ($CO_2 + H_2 \rightarrow CO + H_2O$, named as RWGS) over Cu/ZnO catalyst have been published, such as those about the kinetics [4], the mechanism [5,6], the support effect [7] and the alkali metal promotion effects [8], problems still remain, for example, why copper is the best catalyst for the FWGS and RWGS? Why FWGS and RWGS are the structural sensitivity reactions over the Cu-based

* Corresponding author.
*E-mail address:* wangguichang@nankai.edu.cn (G. Wang).

0166-1280/03/$ - see front matter © 2003 Elsevier B.V. All rights reserved.
doi:10.1016/S0166-1280(03)00209-4

catalyst? In addition, it is also unknown the nature of the FWGS and RWGS reactions are easily poisoned by sulphur.

The water gas shift reaction has been studied over the high-surface-area catalyst containing Cu and ZnO, as well as over a Cu single crystal model catalyst, which has a very well controlled surface cleanness and geometric structure. Those studies showed that the kinetics over pure, single-crystal Cu (111) and Cu (110) are very similar to the kinetics over high-surface-area Cu/ZnO, when compared on a 'per Cu surface atom' basis, and that the activity increases with increasing Cu-surface-area [9,10]. This indicates that metallic Cu provides the active site for catalysis. In the present work, we using the single-crystal metal surfaces such as Cu (111), Cu (100), Cu (110) as well as the sulphur modified Cu (111) surface to model the catalysts for FWGS reaction and RWGS reaction, and then calculating the activation energies of each elementary step based on the Unity Bond Index-Quadratic Exponential Potential (UBI-QEP) approach [11–30]. At last, by comparing the energetic difference of elementary reactions involved in the FWGS reaction and RWGS reaction over different catalysts to explain the above kinetic properties.

## 2. Reaction mechanism for FWGS reaction and RWGS reaction

The mechanism of the water gas shift reaction is not yet completely certain. Some authors support a 'formate mechanism', whereby surface hydroxyls (OH(s)) produced from the dissociation of adsorbed $H_2O$ combine with adsorbed CO (CO(s)) to produce a surface formate intermediate (HCOO(s)), which then decomposes to $H_2$ and $CO_2$. Other authors favor a 'surface redox' mechanism, whereby $H_2O$ dissociatively adsorbs to produce oxygen adatoms (O(s)) and $H_2$, following by the well-known reaction of CO(s) with O(s) to produce $CO_2$. In general, the 'surface redox' mechanism is regarded as the most suitable mechanism for the WGS reaction at low temperatures [31–33], and can be summarized as mechanism A:

$$H_2O(g) \rightarrow H_2O(s) \quad (1A)$$

$$H_2O(s) \rightarrow OH(s) + H(s) \quad (2A)$$

$$OH(s) \rightarrow H(s) + O(s) \quad (3A)$$

$$2H(s) \rightarrow H_2(g) \quad (4A)$$

$$CO(g) \rightarrow CO(s) \quad (5A)$$

$$CO(s) + O(s) \rightarrow CO_2(s) \quad (6A)$$

$$CO_2(s) \rightarrow CO_2(g) \quad (7A)$$

where the subscript 'g' refers to the gas state and 's' to the adsorbed species. In the present paper, we assume that the WGS reactions over different metals (i.e. Cu (111), Cu (100), Cu (110) and Au (111)) obey the same mechanism.

For the RWGS reaction mechanism (named as mechanism B), it can be obtained from the micro-reversible theory:

$$CO_2(g) \rightarrow CO_2(s) \quad (1B)$$

$$CO_2(g) \rightarrow CO_2(s) \quad (2B)$$

$$H_2(g) \rightarrow H_2(s) \quad (3B)$$

$$H_2(s) \rightarrow 2H(s) \quad (4B)$$

$$H(s) + O(s) \rightarrow OH(s) \quad (5B)$$

$$OH(s) + H(s) \rightarrow H_2O(s) \quad (6B)$$

$$H_2O(s) \rightarrow H_2O(g) \quad (7B)$$

In the present study, we assume that the RWGS reaction has the above reaction mechanism.

## 3. Calculation approach of activation barrier

In general, the activation energy of an elementary step can be obtained by a strictly theoretical method like ab initio quantum chemistry method, but it is almost impossible for the complex surface reaction since the expensive computing time required. To avoid this problem, a general and effective approach for analyzing the mechanism of heterogeneously catalyzed reactions has been developed by Shustorovich [11,13], and lately reformulated without the assumptions of Morse potential by Sellers et al. [23]. The approach, based on the Unity Bond Index-Quadratic Exponential Potential (UBI-QEP) method, has provided a rather detailed understanding of reactions such as the hydrogenation of CO to $CH_4$ and $CH_3OH$, Fisher–Tropsch synthesis, and the synthesis and decomposition of $NH_3$. The UBI-QEP

method is a phenomenological approach based on two well-defined assumptions. The first is that the interaction between an atom in an adsorbate and an atom contained in a metal surface is described by a Quadratic-Exponential-Potential. The depth of equilibrium potential wall is related to the atom heat of chemisorption at zero coverage. The effect of a deviation from the equilibrium bond distance for an adatom-metal atom pair is described in terms of the Pauling type bond order relation. The second assumption of the UBI-QEP method is that the sum of partial bond order for an adatom interacting with two or more metal centers and other atoms in the adsorbate is conserved. The UBI-QEP method then yields straightforwardly the heats of chemisorption, $Q$, for molecular and radical species, and the activation energy, $E^*$, for elementary reactions such as dissociation, recombination, and disproportionation.

One should comment on the UBI-QEP analysis of the surface reactivity. In the Arrhenius form of reaction rate constant $k$, $k = A\exp(-E^*/RT)$, $A$ is the pre-exponential factor and the $E^*p$ is the activation energy (barrier). Because of exponential effect, the values of $E^*$ are usually more critical, and the UBI-QEP method deals just with them. In the UBI-QEP analysis, two reactions are compared by the values of $E^*$, ignoring deference in the values of $A$. Thus, the analysis is best justified for a given reaction on a given surface, says fcc (111), but of being two different metals, say Ag (111) and Cu (111). The next best case will be for two reactions of the same reaction order on a given surface, particularly for the reactions of desorption versus dissociation of an adsorbed molecular $AB^*$.

It should be stressed that the activation energies, $E^*$, calculated by UBI-QEP method were strongly effected by the surface coverage and coadsorption [11,23]. In the present study, we intend to study the effect of sulphur on the activity of FWGS reaction and RWGS reaction by comparing the activation barrier difference of each elementary reaction over clear Cu and sulphur-covered Cu surfaces (the model, see Fig. 1).

## 4. Results and discussion

As we know, the chemisorption heat depends on the surface coverage. In this work, we assume that the chemisorption heat of sulphur varies with the change of surface coverage, that is, set $Q^* = Q_0$ at $\theta \leq 0.25$ and set $Q^* = 0.75Q_0$ when $\theta = 0.50$ for fcc (100) (where the $Q_0$ is the atom chemisorption heat of sulphur at zero coverage). According to the scheme of UBI-QEP method, the chemisorption heats of various species involved in the WGS reaction ('surface redox') at different sulphur coverage were calculated and listed in Table 1 (the detailed information of the calculation see Appendices A and B). It can be seen from Table 1 that the chemisorption heat on the sulphur-modified Cu surface is smaller than that on clean Cu surface and it decreases with the increasing of sulphur coverage (esp. for the hollow site), this can be attribute to the co-adsorption effect. Table 2 lists the intrinsic activation barriers of elementary steps for forward ($\Delta E_f^*$) and reverse ($\Delta E_{,r}^*$) directions over Cu (111), Cu (100) and Cu (110) surfaces. Table 3 lists the intrinsic activation barriers of elementary steps over Cu (111) surface for forward ($\Delta E_f^*$) and reverse ($\Delta E_{,r}^*$) directions at different coverages of sulphur. In order to test the reliability of the UBI-QEP method,

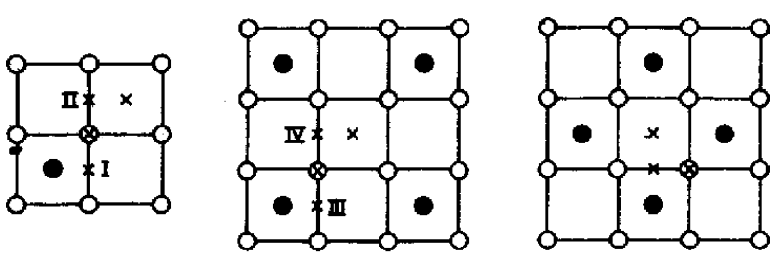


(a) θ=0.125 (b) θ=0.25 (c) θ=0.50

Fig. 1. Models used in the calculation of the heats of chemisorption. ( ∗ ) Possible coordination sites ( × ) for an atom A or a molecule AB coadsorbed with a modifier D (●, i.e. sulphur atom in this paper) in hollow positions of a fcc (100) surface. Metal atoms are shown as open circles. $\theta$ is the surface coverage of sulphur.

Table 1
Heats of chemisorption ($Q$) and total bond energies in gas-phase (D) over Cu (111) for various species at different coverage of sulphur (unit: kJ/mol)

| Species | $D_{AB}$ | $Q$ ($\theta = 0$) | $Q^*$ ($\theta = 0.125$) | | | | $Q^*(\theta = 0.25)$ | | | $Q^*(\theta = 0.50)$ | | |
|---|---|---|---|---|---|---|---|---|---|---|---|---|
| | | | T | $B_1$ | $B_2$ | H | T | B | H | T | B | H |
| H | – | 234 | 112 | 155 | 178 | 212 | 112 | 155 | 147 | 111 | 148 | 106 |
| O | – | 431 | 228 | 329 | 349 | 408 | 228 | 329 | 340 | 231 | 333 | 330 |
| OH | 427 | 218 | 102 | 141 | 164 | 197 | 102 | 141 | 132 | 101 | 133 | 87 |
| $H_2$ | 435 | 21 | 8 | 4 | 13 | 17 | 8 | 4 | 2 | – | – | – |
| $CO_2$ | 1607 | 21 | 8 | 4 | 13 | 17 | 8 | 4 | 2 | – | – | – |
| $H_2O$ | 920 | 58 | 37 | 25 | 42 | 48 | 37 | 25 | 15 | 25 | – | – |
| CO | 920 | 50 | 29 | 19 | 35 | 40 | 29 | 19 | 11 | 17 | – | – |
| S | – | 367 | – | – | – | – | – | – | – | – | – | – |

Sources of experimental values of $Q_H$, $Q_O$, $Q_S$ and $D_{AB}$ are all from Refs. [13,23]. T, B1, B2, B and H stand for the sites on-top, bridge I, bridge II, bridge III (or bridge IV), and hollow site, respectively.

some experimental data are also listed in Tables 4 and 5. As can be seen, the differences between calculated and experimental values $Q$ and $\Delta E^*$ are in the range of 0–12 kJ/mol.

### 4.1. Determining the rate controlling step in the 'surface redox' mechanism

For the FWGS reaction, from Table 2 one can see that the highest energy step is the step of (2A) (106 kJ/mol), which is much higher than other steps. So, we can say that the dissociation of adsorbed $H_2O$ is the rate-controlling step in the 'surface redox' mechanism for the FWGS reaction [8]. For the reverse water gas shift reaction, the step with the highest activation barrier (117 kJ/mol) is the step of (2B), the dissociation of adsorbed $CO_2$, and it is much higher than other steps also, suggesting that the (2B) is the rate controlling step for RWGS reaction in the mechanism B. Those are in perfect agreement with the experimental results [34,35].

### 4.2. Why Cu is more active than Au in FWGS reaction and RWGS reaction?

Since the (2A) and (2B) are the rate controlling steps for the FWGS reaction and RWGS reaction, then we can use the activation barrier of rate controlling step to determine the activity of the FWGS and RWGS reaction directly. From Table 2, we find that the activation barrier of (2A) over the Au (111) surface is higher than that of in Cu (111) surface, which means that the activity of FWGS reaction is higher than the activity of FWGS reaction in Au (111)

Table 2
Intrinsic activation barriers of elementary steps for forward ($\Delta E_f^*$) and reverse ($\Delta E_{,r}^*$) directions over Cu (111),Cu (100), Cu (110) and Au (111) surfaces (unit: kJ/mol)

| Reactions | Cu (111) | | Cu (100) | | Cu (110) | | Au (111) | |
|---|---|---|---|---|---|---|---|---|
| | $\Delta E_f^*$ | $\Delta E_{,r}^*$ | $\Delta E_f^*$ | $\Delta E_{,r}^*$ | $\Delta E_f^*$ | $\Delta E_{,r}^*$ | $\Delta E_f^*$ | $\Delta E_{,r}^*$ |
| $H_2O(g) \rightarrow H_2O(s)$ | 0 | 58 | 0 | 58 | 0 | 58 | 0 | 38 |
| $H_2O(s) \rightarrow OH(s) + H(s)$ | 106 | 6 | 96 | 24 | 89 | 26 | 150 | 0 |
| $OH(s) \rightarrow O(s) + H(s)$ | 65 | 87 | 60 | 99 | 57 | 106 | 71 | 67 |
| $2H(s) \rightarrow H_2(g)$ | 64 | 30 | 79 | 22 | 88 | 17 | 73 | 23 |
| $CO(g) \rightarrow CO(s)$ | 0 | 50 | 0 | 5 | 0 | 5 | 0 | 42 |
| $CO(s) + O(s) \rightarrow CO_2(s)$ | 45 | 117 | 45 | 96 | 45 | 83 | 38 | 234 |
| $CO_2(s) \rightarrow CO_2(g)$ | 21 | 0 | 21 | 0 | 21 | 0 | 25 | 0 |

The $Q_H$, $Q_O$ in the Au (111) surface are abstracted from Refs. [13,23].

Table 3
Intrinsic activation barriers of elementary steps over Cu (111) surface for forward ($\Delta E_f^*$) and reverse ($\Delta E_{,r}^*$) directions at different coverages of sulphur (unit: kJ/mol)

| Reactions | $\theta = 0.125$ | | $\theta = 0.25$ | | $\theta = 0.50$ | |
|---|---|---|---|---|---|---|
| | $\Delta E_f^*$ | $\Delta E_{,r}^*$ | $\Delta E_f^*$ | $\Delta E_{,r}^*$ | $\Delta E_f^*$ | $\Delta E_{,r}^*$ |
| $H_2O(g) \rightarrow H_2O(s)$ | 0 | 48 | 0 | 37 | 0 | 25 |
| $H_2O(s) \rightarrow OH(s) + H(s)$ | 132 | 0 | 234 | 0 | 238 | 0 |
| $OH(s) \rightarrow O(s) + H(s)$ | 72 | 68 | 89 | 17 | 92 | 10 |
| $2H(s) \rightarrow H_2(g)$ | 39 | 50 | 0 | 125 | 0 | 138 |
| $CO(g) \rightarrow CO(s)$ | 0 | 40 | 0 | 29 | 0 | 17 |
| $CO(s) + O(s) \rightarrow CO_2(s)$ | 36 | 137 | 27 | 198 | 0 | 204 |
| $CO_2(s) \rightarrow CO_2(g)$ | 17 | 0 | 8 | 0 | 0 | 0 |

surface (which in good agreement with the experimental results [36]). Similar, for the RWGS reaction, the activation barrier of step (2B) over the Au (111) is higher than that of in Cu (111) surface, and the difference (117 kJ/mol) is higher than that of the FWGS reaction (44 kJ/mol), suggesting that the Cu-based catalyst is more suitable for the RWGS reaction as compared to the metal Au.

### 4.3. Exploring the structure sensitivity of FWGS and RWGS reactions

From Table 2 one can see that the activation barrier of step (2A), the dissociation of adsorbed $H_2O$, decreases in the order of Cu (111) > Cu (100) > Cu (110). Because of the step 2 is the rate-controlling step in the FWGS reaction mechanism, this means that the activity of FWGS reaction is different in the different single copper surfaces; that is to say, the FWGS reaction is a structural sensitivity reaction. For the RWGS reaction, the activation barrier of step (2B) (the rate controlling step in the RWGS reaction mechanism) decreases in the same order as that of (2A), suggesting that the RWGS is a structure sensitivity reaction also. In addition, we find that the activation barrier difference of step (2B) over different Cu surface is higher than that of (2A) at different Cu surfaces. So, it may be concluded that the RWGS reaction is a more structural sensitivity reaction when compared with the FWGS reaction. For this reason, it may be explained as follows: for the RWGS reaction, the controlling step is the dissociation of C–O bond in $CO_2$, and the FWGS reaction is the dissociation of the H–O bond in $H_2O$. Since the C–O bond is stronger as compared to the O–H bond, then it may be more structure dependence on the surface structure, i.e. the more open surface such as Cu (110), the easier to be broken.

It should be pointed that in the above discussion, we let the $n$ in the equation of $Q_A = Q_{0A}(2 - 1/n)$ equals to 5 for Cu (110) surface is merely a estimation (Appendix A), and the more exactly date for the atomic adsorption energies of oxygen at Cu (111), Cu (100) and Cu (110) surfaces should be carried out by the first-principle quantum chemistry method.

Table 4
Calculated heats of adsorption (Q) comparison with experiment data

| | Surface | $Q$ (kJ/mol) | | Ref. |
|---|---|---|---|---|
| | | Calcd | Exp. | |
| $H_2O$ | Cu (111) | 59 | 59 | 17 |
| $CH_3OH$ | Cu (111) | 63 | 71 | 17 |
| $CO_2$ | Cu (111) | 21 | 21 | 17 |

Table 5
Calculated activation barriers ($\Delta E^*$) comparisons with experiment data

| Reaction | Surface | $\Delta E^*$ (kJ/mol) | | Ref. |
|---|---|---|---|---|
| | | Calcd | Exp. | |
| $H_2O \rightarrow OH + H$ | Cu (111) | 109 | 114 | 31 |
| $O + H \rightarrow OH$ | Cu (111) | 86 | 92 | 17 |
| $CO + O \rightarrow CO_2$ | Pd (111) | 100 | 105 | 17 |
| $OH + H \rightarrow HCOO$ | Rh (100) | 42 | 33 | 17 |
| $CH_3O + H \rightarrow CH_3OH$ | Rh (111) | 56 | 58 | 20 |

### 4.4. The influence of sulphur on the activity of FWGS and RWGS

From Table 3 one can find that the activation barrier of step (2A) increases with the increasing of the surface coverage of sulphur (from 106 to 238 kJ/mol when the coverage increases from $\theta = 0.0$ to 0.5), and the activity of the RWGS reaction will decreases in the same order. Similarly, the activation barrier of step (B2) increases with the increasing of the coverage of sulphur also, suggesting that the activity of the RWGS reaction will

also decreased as the copper surface is covered with the sulphur atom. Moreover, we think that may be the dominating reason of the FWGS reaction and RWGS reaction is easily poisoned by the sulphur. Of course, the reasons for the sulphur poison are very complex, and the above explanation is only one aspect of the electronic effect.

By the way, the above study is based on the Cu (111) surface only, and for the Cu (100) as well as Cu (110) surface can also be discussed by the same way, and the results is similar, i.e. the activation energy of the controlling step increases with the increasing the coverage of sulphur.

## 5. Conclusion

By the above analysis, we can gain the following results:

(1) For the FWGS reaction, the rate-controlling step is the dissociation of adsorbed $H_2O$, and the dissociation of adsorbed $CO_2$ is the rate-controlling step for the RWGS reaction.
(2) Both of the FWGS reaction and the RWGS reaction are structural sensitivity reactions over Cu-based catalyst, and the RWGS reaction is much more structural sensitivity than that of the FWGS reaction.
(3) The activity of FWGS and RWGS reaction over Cu (111) is higher than the activity over Au (111) surface, and the difference is larger for the RWGS reaction.
(4) The activation barrier of rate controlling step in FWGS and RWGS reaction increases with the increasing of the surface coverage of sulphur, and this may be the reason why the FWGS reaction and RWGS reaction is easily poisoned by the sulphur.

In this paper, we just using the UBI-QEP method to analyze the kinetic properties of FWGS reaction and RWGS reaction by comparing the energy differences simultaneously, the mode is crude, and a more quantitative method such as quantum chemistry [37,38] and computer simulation [39–42] should be developed.

## Acknowledgements

This work was supported by National Natural Science Foundation (No.20273034)), the foundation of State Key Laboratory of Coal conversion and the State Key Laboratory of $C_1$ Chemistry and Technology (Taiyuan University of Technology) of China.

## Appendix A. The formulas for calculating the heat of adsorption and the activation barriers [11,23]

### A.1. Heat of adsorption

$$Q_A = Q_{0A}(2 - 1/n) \qquad \text{(the heat adsorption of atom)}$$

For the fcc Cu (111), Cu (100) and Cu (110), we assume that the $n = 3$, 4 and 5, respectively, based on the surface atom density increasing in the order of Cu (111) > Cu (100) > Cu (110).

$$Q_{AB} = Q_A^2/(Q_A + D_{AB}) \qquad \text{(strong adsorption)}$$

$$Q_{AB} = Q_{0A}^2/((Q_{0A}/n) + D_{AB}) \qquad \text{(weak adsorption)}$$

$$Q_{AB} = 0.5(Q_A^2/(Q_A + D_{AB}) + Q_{0A}^2/((Q_{0A}/n) + D_{AB}))$$

(middle adsorption)

### A.2. Activation barrier

(1) $AB_{g,(s)} = A_S + B_S$

$$E_{AB,g} = 0.5(D_{AB} + Q_A Q_B/(Q_A + Q_B) - Q_{AB} - Q_A - Q_B)$$

$$E_{AB,s} = 0.5(D_{AB} + Q_A Q_B/(Q_A + Q_B) + Q_{AB} - Q_A - Q_B)$$

(2) $A_S + B_S = AB_S$

$$E_{A-B,g} = E_{A-B,s} = Q_A + Q_B - D_{AB} + E_{AB,g},$$

if $E_{AB,g} > 0$

$$E_{A-B,g} = E_{A-B,s} - E_{AB,g} = Q_A + Q_B - D_{AB},$$

if $E_{AB,g} < 0$

$$E_{A-B,s} = Q_A Q_B/(Q_A + Q_B)$$

(for the one dimension reaction, such as $CO_S + O_S = CO_{2S}$)

(3) $X_S + Y_S = Z_S + F_S$

$$E_{XY(S)} = 0.5(D_X + D_Y - D_Z - D_F + Q_Z Q_F/(Q_Z + Q_F) + Q_X + Q_Y - Q_Z - Q_F)$$

$$(D = D_X + D_Y - D_Z - D_F > 0)$$

## Appendix B. Coverage and coadsorption effect [8,11,23]

Here are the formulas for calculating the heats of chemisorption of species at different coverage of sulphur (Fig. 1):

### *B.1. Atom coadsorption [11,23]*

(A) For the case of (a) in Fig. 1, (i.e. $\theta = 0.125$):

(a) The heat of chemisorption of A atom on top site ($h = 4/7$) is

$$Q_A^* = Q'_{A,D} \tag{B1}$$

where

$$Q'_{A,D} = Q_A h[1 - (1 + 4h/r)^{-2}] \tag{B2}$$

and

$$r = Q_D/Q_A \tag{B3}$$

where $Q_D$ is the heat of chemisorption of oxygen at $\theta = 0.125$;

(b) The heat of chemisorption of A atom on bridge site I ($h = 3/7$) is

$$Q_A^* = 2Q'_{A,D} \tag{B4}$$

where $Q'_{A,D}$ can be obtained by Eq. (B2);

The heat of chemisorption of A atom on bridge site II ($h = 3/7$) is

$$Q_A^* = Q'_{A,D} + 3Q_A/7 \tag{B5}$$

where $Q'_{A,D}$ can be obtained by Eq. (B2);

(c) The heat of chemisorption of A atom on the hollow site ($h = 1/4$) is

$$Q_A^* = Q'_{A,D} + 3Q_A/4 \tag{B6}$$

where $Q'_{A,D}$ can be obtained by Eq. (B2);

(B) For the case of (b) in Fig. 1(i.e. $\theta = 0.25$):

(a) The heat of chemisorption of A atom on top site ($h = 4/7$) can be calculated by Eq. (B1) and $Q_D$ in Eq. (B3) is the heat of chemisorption of oxygen at $\theta = 0.25$;

(b) The heat of chemisorption of A atom on bridge site III ($h = 3/7$) or on bridge site IV ($h = 3/7$) can be calculated by Eq. (B4) and $Q_D$ in Eq. (B3) is the heat of chemisorption of oxygen at $\theta = 0.25$;

(c) The heat of chemisorption of A atom on the hollow site ($h = 1/4$) is

$$Q_A^* = 4Q'_{A,D} \tag{B7}$$

where $Q'_{A,D}$ can be obtained by Eq. (B2) and $Q_D$ in Eq. (B3) is the heat of chemisorption of oxygen at $\theta = 0.25$;

(C) For the case of (c) in Fig. 1 (that is $\theta = 0.50$):

(a) The heat of chemisorption of A atom on top site ($h = 4/7$) can be calculated by Eq. (B1) and $Q^*_{A,D}$ can be obtained by Eq. (B8)

$$Q'_{A,D} = Q_A h[1 - 4(1 + 8h/r)^2]. \tag{B8}$$

and $Q_D$ in Eq. (B3) is the heat of chemisorption of oxygen at $\theta = 0.50$;

(b) The heat of chemisorption of A atom on bridge site III ($h = 3/7$) or on bridge site IV ($h = 3/7$) can be calculated by Eq. (B4) and $Q^*_{A,D}$ can be obtained by Eq. (B8);

(c) The heat of chemisorption on the hollow site ($h = 1/4$) can be obtained by Eq. (B7) and $Q^*_{A,D}$ can be obtained by Eq. (B8).

As an example, we calculate the heats of chemisorption of H atom at different coverage of sulphur using the above formulas:

(1) For the case of (a) in Fig. 1, i.e. $\theta = 0.125$, $r = Q_D/Q_A = 367/234 = 1.57$ (where 367 is the heat

of chemisorption of sulphur at $\theta = 0.125$), then the heats of chemisorption of H atom at different positions for the case of $\theta = 0.125$ are $Q^*$(on-top) $= Q'_{A,D} = Q_A h[1 - (1 + 4h/r)^{-2}] = 112$ kJ/mol (where $h = 4/7$), $Q^*$(on bridge I) $= 2Q'_{A,D} = 155$ kJ/mol (where $h = 3/7$), $Q^*$(on bridge II)$= Q'_{A,D} + 3Q_A/7 = 178$ kJ/mol (where $h = 3/7$), and $Q^*$(on hollow site) $= Q'_{A,D} + 3Q_A/4 = 212$ kJ/mol (where $h = 1/4$), respectively.

(2) For the case of (b) in Fig. 1, i.e. $\theta = 0.25$, $r = Q_D/Q_A = 367/234 = 1.57$ (where 367 is the heat of chemisorption of sulphur at $\theta = 0.25$), then the chemisorption heats of H atom at different sites for the case of $\theta = 0.25$ are $Q^*$(on-top) $= Q'_{A,D} = Q_A h[1 - (1 + 4h/r)^{-2}] = 112$ kJ/mol (where $h = 4/7$), $Q^*$(on bridge III or IV) $= 2Q'_{A,D} = 155$ kJ/mol (where $h = 3/7$), and $Q^*$(on hollow site) $= 4Q'_{A,D} = 147$kJ/mol (where $h = 1/4$), respectively.

(3) For the case of (c) in Fig. 1, i.e. $\theta = 0.50$, $r = Q_D/Q_A = 275/234 = 1.38$ (where 275 is the heat of chemisorption of sulphur at $\theta = 0.50$), then the chemisorption heats of H atom at different sites for the case of $\theta = 0.50$ are $Q^*$(on-top) $= Q'_{A,D} = = Q'_{A,D} = Q'_{A,D} = Q_A h[1 - 4(1 - 8h/r)^2] = 111$ kJ/mol (where $h = 4/7$), $Q^*$(on bridge III or IV) $= 2\ Q'_{A,D} = 148$ kJ/mol, and $Q^*$(on hollow site) $= 4\ Q'_{A,D} = 106$ kJ/mol (where $h = 1/4$), respectively.

### *B.2. Molecular coadsorption [11,23]*

The formulas for calculating the heats of chemisorption are the same as the atom coadsorption except that the $h = 1$, 1/2 and 1/4 for the top, bridge and hollow sites, respectively.

## References


[1] D.S. Newsome, Catal. Rev. Engng 21 (1980) 275.
[2] H. Bohlbro, M.H. Jorgensen, Chem. Engng World 5 (1970) 46.
[3] R. Habermehl, K. Atwood, Am. Chem. Soc., Div. Fuel Chem. Prepr. 8 (1964) 10.
[4] G.C. Chinchen, M.S. Spencer, K.C. Waugh, D.A. Whan, J. Chem. Soc., Faraday Trans. 1 83 (1987) 2183.
[5] T. Salmi, R. Hakkarainen, Appl. Catal. 49 (1989) 282.
[6] E. Fiolitakis, H. Hofman, J. Catal. 80 (1983) 328.
[7] S. Kinnaird, G. Webb, G.C. Chinchen, J. Chem. Soc., Faraday Trans. 1 83 (1987) 3399.
[8] J. Nakamura, J.M. Campbell, C.T. Campbell, J. Chem. Soc. Faraday Trans. 1 86 (1990) 2725.
[9] C.T. Campbell, K.A. Daube, J. Catal. 104 (1987) 109.
[10] Q.R. Cai, S.Y. Peng, The Catalysis Processes in $C_1$ Chemistry, Beijing Industry Press, Beijing, 1995, Chapter 2, in Chinese.
[11] E. Shustorovich, Surf. Sci. Rep. 6 (1986) 1.
[12] E. Shustorovich, Surf. Sci. 175 (1986) 561.
[13] E. Shustorovich, Adv. Catal. 37 (1990) 101.
[14] A.T. Bell, E. Shustorvich, J. Catal. 121 (1990) 1.
[15] E. Shustorvich, A.T. Bell, Surf. Sci. 278 (1991) 359.
[16] E. Shustorvich, A.T. Bell, Surf. Sci. 259 (1991) L791.
[17] E. Shustorovich, A.T. Bell, Surf. Sci. 253 (1991) 386.
[18] E. Shustorovich, A.T. Bell, Surf. Sci. 279 (1992) 355.
[19] P.P. Olivera, E.M. Patrito, H. Sellers, Surf. Sci. 313 (1994) 25.
[20] P.P. Olivera, E.M. Patrito, H. Sellers, Surf. Sci. 327 (1995) 330.
[21] H. Sellers, E. Shustorovich, Surf. Sci. 356 (1996) 209.
[22] H. Sellers, E. Shustorovich, J. Mol. Catal. A: Chem. 119 (1997) 367.
[23] E. Shustorovich, H. Sellers, Surf. Sci. Rep. 31 (1998) 1.
[24] G.C. Wang, Y.Z. Zhao, Z.S. Cai, et al., Surf. Sci. 465 (2000) 51.
[25] F. Gobal, S. Azizian, J. Chem. Res. (1997) 324.
[26] F. Gobal, S. Azizian, Langmuir 13 (1999) 5999.
[27] S. Azizian, F. Gobal, J. Mol. Catal. 153 (2000) 191.
[28] F. Gobal, S. Azizian, J. Mol. Catal. 136 (1998) 169.
[29] M.J. Hei, H.B. Shen, J.Y. Yi, J. Lin, G. Wei, D.W. Liao, Surf. Sci. 417 (1998) 82.
[30] B.R. Shen, X.Y. Chen, K.N. Fan, J.F. Deng, Surf. Sci. 408 (1998) 128.
[31] Y.B. Cui, X.Z. Wang, Y.H. Sun, B. Zhong, J. Natural Gas Chem. (Chin.) 6 (1997) 121.
[32] R.C. Boundary, G.T. Hutchings, A.M. Wand, Catal. Today 23 (1995) 43.
[33] T.S. Askgard, J.K. Norskov, V.C. Ovesen, P. Stoltze, J. Catal. 156 (1995) 229.
[34] K.H. Ernst, C.T. Campbell, G. Moretti, J. Catal. 134 (1992) 66.
[35] S.J. Fujita, M. Suui, N. Takezawa, J. Catal. 134 (1992) 220.
[36] D.C. Grenoble, M.M. Estadt, D.F. Ollis, J. Catal. 67 (1980) 90.
[37] G.C. Wang, L. Jiang, Z.S. Cai, Y.M. Pan, N.J. Guan, Y. Wu, X.Z. Zhao, Y.W. Li, Y.H. Sun, B. Zhong, J. Mol. Struct. (THEOCHEM) 371 (2002) 589–590.
[38] G.C. Wang, L. Jiang, Z.S. Cai, Y.M. Pan, X.Z. Zhao, W. Huang, K.C. Xie, Y.W. Li, Y.H. Sun, B. Zhong, J. Phys. Chem. B 107 (2003) 557.
[39] J.A. Dumesic, D.F. Rudd, L.M. Aparicio, J.E. Rekoske, The Microkinetics of Heterogeneous Catalysis, American Chemical Society, Washington, DC, 1993.
[40] P. Stoltz, Prog. Surf. Sci. 65 (2000) 63.
[41] G.C. Wang, Y.B. Cui, Y.H. Sun, B. Zhong, J. Mol. Catal. (China) 12 (1998) 41.
[42] W.S. Yang, H.W. Xiang, Y.W. Li, Y.H. Sun, Catal. Today 61 (2000) 237.